JOURNAL OF CATALYSIS 49, 332–344 (1977)

An Infrared Study of NO and CO Adsorption on a Silica-Supported Ru Catalyst

ANATOLI A. DAVYDOV[1] AND ALEXIS T. BELL

Materials and Molecular Research Division, Lawrence Berkeley Laboratory, and Department of Chemical Engineering, University of California, Berkeley, California 94720

Received December 31, 1976; revised April 14, 1977

Infrared spectra were obtained for NO and CO adsorbed on reduced and oxidized Ru supported on silica. Adsorption of NO on a fully reduced sample produced bands at 1810 and 1860 cm^{-1}. With prolonged catalyst exposure to NO, the latter band shifted to higher frequencies. Spectra of NO adsorbed on an oxidized sample showed only a single band at 1880 cm^{-1}. Both the band at 1810 cm^{-1} and that occurring between 1860 and 1880 cm^{-1} are assigned to NO adsorbed as NO^+. The low frequency band is associated with adsorption on partially oxidized Ru sites and the high frequency band with adsorption on more fully oxidized sites. On a fully reduced sample, CO adsorption produced a single band at 2040 cm^{-1} which is assigned to linearly bonded CO. Oxidation of Ru and subsequent adsorption of CO produced bands at 2130 and 2070 cm^{-1}. This pair of bands is assigned to the symmetric and asymmetric stretches of two CO molecules bonded to a single oxidized Ru site.

INTRODUCTION

Ruthenium is an active catalyst for the reduction of NO by CO, and, hence, it is desirable to learn as much as possible about the structures formed when these molecules adsorb. A useful tool for this purpose is infrared spectroscopy since it can reveal information concerning the form of adsorption, the stability of the adsorbed structure, and the influence of various surface pretreatments.

A number of infrared studies concerning CO adsorbed on Ru have been reported previously. Lynds (*1*) observed two bands at 2151 and 2083 cm^{-1} for Ru supported on silica and at 2125 and 2060 cm^{-1} for Ru supported on alumina. Guerra and Schulman (*2*) identified two broad bands for CO adsorbed on silica-supported Ru. The band occurring between 2010 and 1990 cm^{-1} was assigned to Ru–CO, while that occurring between 1910 and 1870 cm^{-1} was assigned to Ru_2CO. Two bands in the region between 2100 and 1900 cm^{-1} were also reported by Kobayashi and Shirasaki (*3*) for Ru supported on silica. These authors did not make specific structural assignments for either band but suggested that both might be attributed to multiple CO adsorption at a single Ru site.

The effect of Ru particle size on the spectrum of CO adsorbed on alumina-supported Ru has recently been discussed by Dalla Betta (*4*). For particles 90 Å in diameter only a single band at 2028 cm^{-1} was observed, while, for particles 60 Å and smaller, three bands in the vicinity of 2140, 2080, and 2040 cm^{-1} was noted. The exact positions and relative intensity of the three bands changed with decreasing particle size. The low-frequency band was

[1] Permanent address: Institute of Catalysis, Novosibirsk, U.S.S.R.

ISSN 0021-9517

assigned to CO adsorbed on low-index planes of Ru, while the two higher-frequency bands were associated with CO adsorbed on low-coordination edge and corner metal atoms. These band assignments have been questioned, however, by Brown and Gonzalez (*5*). Based upon their own studies performed with silica-supported Ru, they noted that CO adsorption on a reduced sample produced a strong band at 2030 cm^{-1} and weak bands at 2150 and 2080 cm^{-1}, whereas CO adsorbed on an oxidized sample produced a strong band at 2080 cm^{-1} and medium intensity bands at 2135 and 2030 cm^{-1}. The low-frequency band was assigned to CO adsorbed as Ru–CO. The high- and medium-frequency bands were assigned to CO adsorbed on a surface oxide and CO adsorbed on a Ru atom perturbed by a nearby oxygen atom, respectively.

In contrast to the effort devoted to adsorbed CO, only two infrared studies have been reported dealing with NO adsorbed on Ru. Unland (*6*) reported bands at 1882, 1861, 1856, and 1715 cm^{-1} for NO adsorbed on alumina-supported Ru. Working with a fully reduced sample of Ru supported on silica Brown and Gonzalez (*7*) observed a single band at 1800 cm^{-1} which shifted to 1815 cm^{-1} upon extended exposure of the sample to NO. These authors assigned the band to a structure of the form $Ru^{\delta-}$–$NO^{\delta+}$.

In the present work infrared spectroscopy was used to examine further the structures formed upon adsorption of CO and NO on silica-supported Ru. The effects of sample pretreatment in either reducing or oxidizing environments were examined. It was established that both CO and NO can adsorb in more than one form and that the strengths of adsorption of these forms differ markedly.

EXPERIMENTAL

A 4% Ru-silica catalyst was prepared by impregnating Cab-O-Sil, Grade HS-5 (Cabot Corp.), with an aqueous solution of $RuCl_3 \cdot 3H_2O$ (Engelhard Industries). The resulting gel was dried in an air oven at 90°C for 1 day. The dried material was then ground, sieved to −325 mesh, and reduced in flowing H_2 (100 cm^3/min) at 1 atm. The reduction temperature was maintained at room temperature for the first 2 hr, increased to 250°C over a period of 2 hr, maintained at 250°C for 2 hr, increased to 320°C for an additional 2 hr, and then slowly reduced to room temperature over a final 2-hr period. Transmission electron micrographs of the reduced catalyst yielded a number-average crystallite size of 26 Å and a surface-area average size of 41 Å.

The H_2 used for catalyst reduction was obtained from the Lawrence Berkeley Laboratory and contained less than 1 ppm of impurities. NO and CO (Matheson Technical Grade) were vacuum distilled and stored in glass bulbs. ^{13}CO (Stohler Isotope Chemicals), 90% enriched in ^{13}C, and ^{15}NO (Stohler Isotope Chemicals), 99% enriched in ^{15}N, were used without additional purification.

The infrared cell was similar to those described by Little (*8*) and was constructed of Pyrex in the form of an inverted T. NaCl windows, attached with Torr-Seal low-vapor pressure resin, were used to cover the openings in the traverse portion of the cell, through which the infrared beam passed. A small furnace was placed around the vertical portion of the cell in order to heat the sample during pretreatment or adsorption. The temperature in this part of the cell was measured with a chromel–alumel thermocouple inserted into the glass thermowell. Introduction and evacuation of gas from the cell was achieved through a side arm closed off by a vacuum stopcock. During sample pretreatment and gas adsorption the cell was attached to a vacuum manifold.

For the infrared studies, about 100 mg of the reduced catalyst was pressed into a

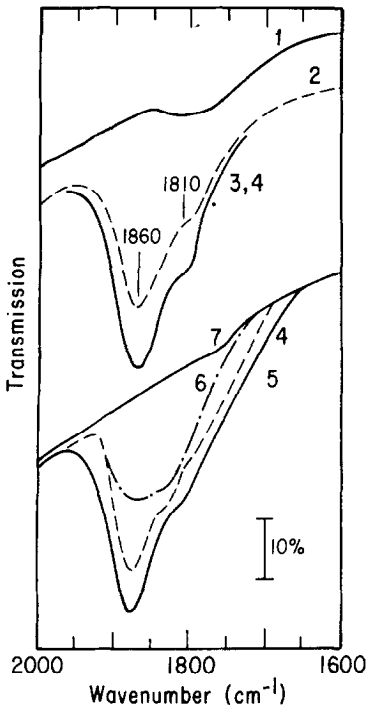

FIG. 1. Spectra of NO adsorbed on Ru pretreated at 300°C following schedule A: (1) background; (2) following adsorption of NO at 10 Torr and 25°C; (3) following adsorption of NO at 100 Torr and 25°C; (4) following evacuation of NO at 25°C; (5) following desorption *in vacuo* at 100°C; (6) following desorption *in vacuo* at 200°C; (7) following desorption *in vacuo* at 300°C.

disk 29 mm in diameter using a pressure of 6000 psi. The catalyst was then mounted in a quartz holder and was placed inside the infrared cell.

Prior to initiating adsorption, the catalyst disk was pretreated by heating under vacuum (10^{-5} to 10^{-6} Torr), reducing with H_2 at 350 Torr, and then further heating under vacuum. Pretreatment temperatures of either 300 or 500°C were used. For each temperature the effects of two pretreatment schedules were explored. For schedule A, the durations of evacuation, reduction, and evacuation were 2 hr each. The corresponding periods for schedule B were 20, 4, and 20 hr, respectively.

Infrared spectra were recorded by placing the cell in the sample compartment of a Perkin–Elmer 467 spectrometer. To compensate for the infrared adsorption of the silica support a second catalyst disk was placed in the reference beam of the spectrometer. This disk was not exposed to the adsorbing gases. Spectra were recorded at room temperature over the range of 3500–1300 cm^{-1}.

RESULTS

Adsorption of NO

Spectrum 2 shown in Fig. 1 is obtained after pretreatment of the catalyst at 300°C following schedule A and subsequent adsorption of NO at 10 Torr and 25°C. Two bands are evident at 1860 and 1810 cm^{-1}. Upon increasing the NO partial pressure to 100 Torr, both bands grow in intensity (spectrum 3). The presence of a gas-phase band at 1876 cm^{-1} in these spectra was eliminated by using a reference cell filled with NO to the same pressure used in the sample cell. For these runs the reference disk consisted of silica. As shown by spectrum 4, evacuation of NO at 25°C does not alter the spectrum. With an increase in the desorption temperature, a progressive decrease in the intensity of both bands is observed (spectra 5–7). These spectra show that the species corresponding to the band at 1860 cm^{-1} is more easily desorbed than that corresponding to the band at 1810 cm^{-1}. Figure 2 shows the effect of heating the catalyst in NO after an initial period of adsorption at 25°C. Spectrum 3 in this figure is essentially the same as spectrum 3 in Fig. 1. After heating at 100°C there is a preferential growth in the high-frequency band and a shift in its position from 1855 to 1870 cm^{-1}. Results similar to those shown in Figs. 1 and 2 were obtained using a sample pretreated at 300°C following schedule B.

NO adsorption on a catalyst sample pretreated at 500°C following schedule B gives rise to the spectra shown in Fig. 3. These spectra closely resemble those shown

in Figs. 1 and 2. It should be noted that, using this sample, heating in NO was carried out at temperatures up to 400°C. At this temperature, the high-frequency band is shifted to 1875 cm^{-1}.

Having established that the temperature and duration of H_2 reduction have little or no effect upon the spectra of adsorbed NO, experiments were conducted to determine the effects of intentional oxidation of the Ru surface. Spectrum 3 in Fig. 4 illustrates the effect of adding 50 Torr of O_2 to a sample previously exposed to 6 Torr of NO. Notice that the high-frequency band greatly increases in intensity and shifts from 1860 to 1880 cm^{-1}. A similar shift in frequency is achieved if the sample is preoxidized in 50 Torr of O_2 at 200°C for 30 min and then exposed to NO. In this case there is no trace of a band at 1810 cm^{-1}.

Adsorption studies were also conducted using ^{15}NO. These experiments gave similar results to those using ^{14}NO, with the exception that the bands at 1860 and 1810 cm^{-1} were shifted to 1825 and 1780 cm^{-1}, respectively.

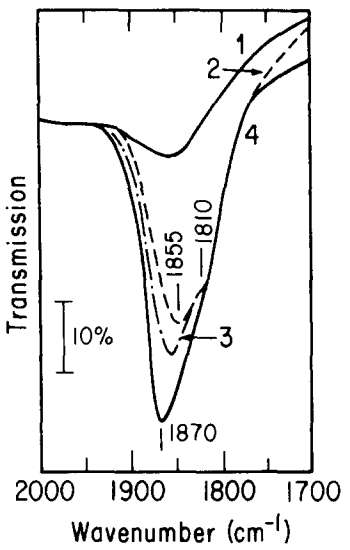

FIG. 2. Spectra of NO adsorbed on Ru pretreated at 300°C following schedule A: (1) background; (2) following adsorption of NO at 0.3 Torr and 25°C; (3) following adsorption of NO at 10 Torr and 25°C; (4) following heating in NO to 100°C.

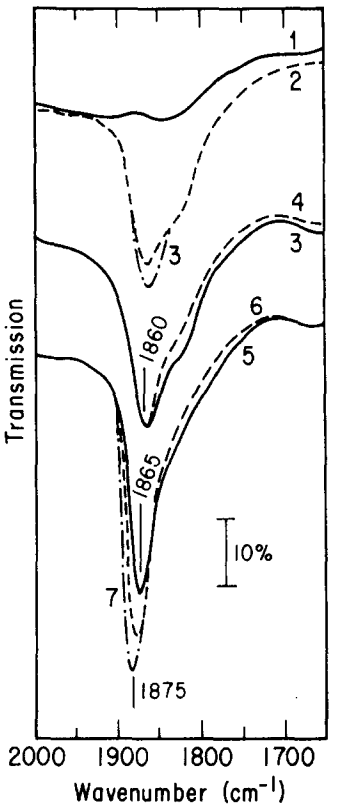

FIG. 3. Spectra of NO adsorbed on Ru pretreated at 500°C following schedule B: (1) background; (2) following adsorption of NO at 0.5 Torr and 25°C; (3) following adsorption of NO at 10 Torr and 25°C; (4) following heating in NO to 100°C; (5) following heating in NO to 200°C; (6) following heating in NO to 300°C; (7) following heating in NO to 400°C.

Adsorption of CO

Adsorption of CO on a sample pretreated at 300°C following schedule A produces the spectra shown in Fig. 5. Three bands are observed at 2145, 2080, and 2040 cm^{-1}. The intensity of the band observed at 2040 cm^{-1} increases slightly as the pressure is raised from 10 to 100 Torr. The effect of adsorbate pressure on the intensities of the bands at 2145 and 2080 cm^{-1} is harder to discern because of the appearance of bands at 2180 and 2110 cm^{-1} associated

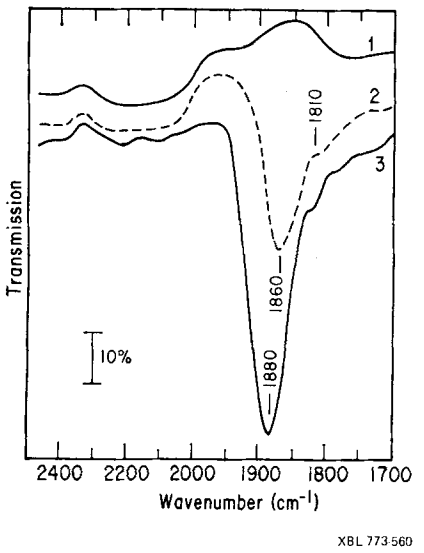

FIG. 4. Spectra of NO adsorbed on Ru pretreated at 300°C following schedule A: (1) background; (2) following adsorption of NO at 6 Torr and 25°C; (3) following addition of 50 Torr of O_2 at 25°C.

with gaseous CO. Nevertheless, comparison of spectra 2, 3, and 5 suggests a modest increase in the intensities of the bands at 2145 and 2080 cm^{-1} with increasing pressure.

Desorption at 25°C leads to a shift of the band located at 2040 and 2030 cm^{-1}, as can be seen in spectrum 1 of Fig. 6. Increasing the desorption temperature to 100°C causes a reduction in the intensity of all three bands and a further shift of the low frequency band to 2010 cm^{-1} (spectrum 2). Finally, upon raising the desorption temperature to 200°C, all three of the bands disappear.

In an effort to identify the effects of catalyst pretreatment on the infrared spectra of adsorbed CO, experiments were carried out in which the pretreatment schedule and temperature were varied. Pretreatment at 300°C following schedule B had little effect on either the frequencies or relative intensities of the three CO bands. Increasing the pretreatment temperature to 500°C caused a significant increase in the intensity of the band at 2040 cm^{-1} relative to the two high-frequency bands (see, for example, spectrum 2 in Fig. 5 and spectrum 2b in Fig. 7). However, as in the case of pretreatment at 300°C, lengthening the pretreatment duration had no influence on the spectrum. Here again, evacuation of the gas phase at 25°C caused a slight downscale shift of the low-frequency band and, in contrast to pretreatment at 300°C, an attenuation of the two high-frequency bands.

Further experiments were conducted to establish the effects of heating the sample in CO. Spectrum 1a in Fig. 7 shows the spectrum of adsorbed CO on a sample pretreated in H_2 at 500°C using schedule A and then heated in CO at 300°C for 30 min. For comparison, a spectrum of CO adsorption on a sample reduced only in H_2 is shown in the lower half of Fig. 7. The spectrum of CO on the CO-treated sample shows only an intense band at 2040 cm^{-1}

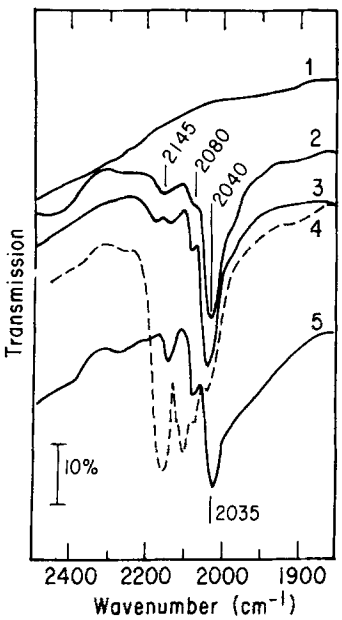

FIG. 5. Spectra of CO adsorbed on Ru pretreated at 300°C following schedule A: (1) background; (2) following adsorption of CO at 10 Torr and 25°C; (3) following adsorption of CO at 60 Torr and 25°C; (4) following adsorption of CO at 100 Torr and 25°C; (5) following evacuation of CO at 25°C.

and two weak bands at 2180 and 2110 cm^{-1}, associated with gas-phase CO. The intensity of the band at 2040 cm^{-1} is noticeably greater on the sample heated in CO. Upon evacuation of the gas phase at 25°C (spectrum 2a), the low-frequency band shifts to 2030 cm^{-1}. A further shift of this band to 2010 cm^{-1} occurs when the desorption temperature is raised to 200°C (spectrum 3a).

To complement the studies performed using fully reduced samples, spectra were recorded on catalyst samples which had been intentionally oxidized. Figure 8 illustrates the spectra obtained on a sample pretreated at 300°C, following schedule A, and then exposed to O_2 at 25°C. Upon adsorption of CO (spectrum 1) only two bands are observed at 2070 and 2130 cm^{-1}. The only evidence for a band at 2040 cm^{-1} is a weak shoulder on the low-frequency side of the band at 2070 cm^{-1}. Evacuation of the CO at 25°C (spectrum 2) causes slight reductions in the intensities of the two bands. Increasing the temperature of O_2 exposure causes several interesting changes. At 200°C (spectrum 4), there is a noticeable increase in the intensities of the bands at 2130 and 2070 cm^{-1} and a total absence of a shoulder at 2040 cm^{-1}. Further increase of the oxidation temperature to 300°C (spectrum 5) causes a reduction in the band intensities due to a decline in the transmittance of the catalyst disk. A similar loss of transmittance due to Ru oxidation has been noted by Brown and Gonzalez (7).

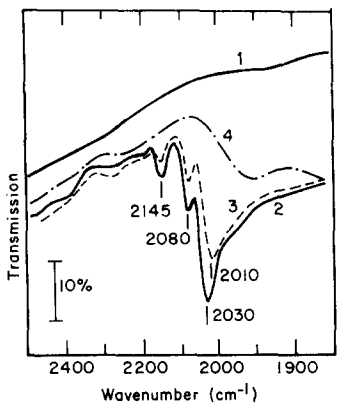

FIG. 6. Spectra of CO adsorbed on Ru pretreated at 300°C following schedule A: (1) background; (2) following adsorption of CO at 100 Torr and 25°C and subsequent evacuation at 25°C; (3) following desorption of CO at 100°C for 1 hr; (4) following desorption of CO at 200°C for 1.5 hr.

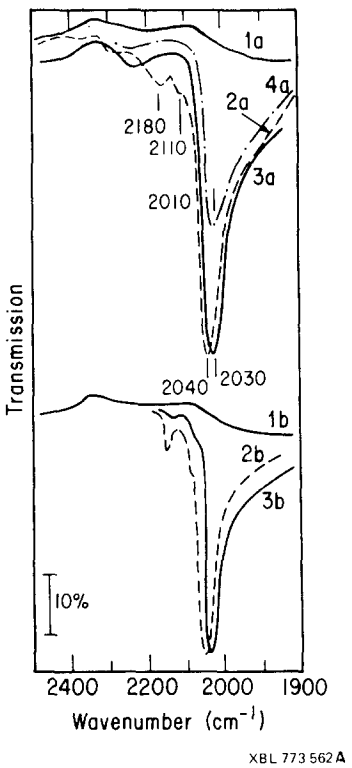

FIG. 7. Spectra of CO adsorbed on Ru: (1a) background; (2a) following pretreatment at 500°C using schedule A, reduction in CO at 300°C, and adsorption of CO at 40 Torr and 25°C; (3a) following evacuation of CO at 25°C; (4a) following desorption *in vacuo* at 200°C; (1b) following pretreatment at 500°C using schedule A; (2b) following adsorption of CO at 10 Torr and 25°C; (3b) following evacuation of CO at 25°C.

Oxidation of the Ru surface by N_2O and NO were also examined. Oxidation by N_2O was accomplished by exposure of the sample to 23 Torr of N_2O at 25°C and subsequent evacuation of the gas phase. Pretreatment in NO was accomplished in a similar fashion, with the additional step

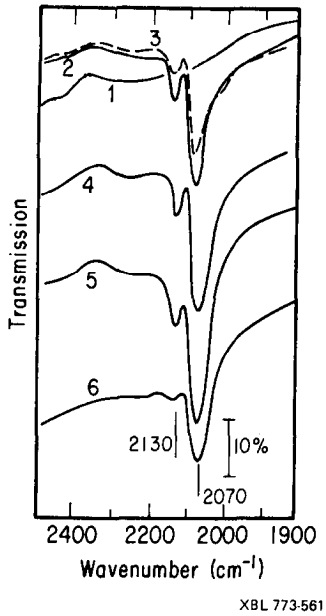

FIG. 8. Spectra of CO adsorbed on Ru pretreated at 300°C following schedule A: (1) background following oxidation in O_2 at 50 Torr and 25°C; (2) following adsorption of CO at 15 Torr and 25°C; (3) following evaluation at 25°C; (4) following oxidation in O_2 at 80 Torr and 100°C, adsorption of CO at 15 Torr and 25°C, and evacuation of CO at 25°C; (5) following oxidation in O_2 at 300 Torr and 200°C, adsorption of CO at 15 Torr and 25°C; (6) following oxidation in O_2 at 300 Torr and 300°C, adsorption of CO at 15 Torr and 25°C, and evacuation of CO at 25°C.

of NO desorption at 300°C. Adsorption of CO on the oxidized samples produces spectra 1a and 1b shown in Fig. 9. In the presence of gas-phase CO, the sample oxidized in N_2O shows three bands occurring at 2130, 2070, and 2040 cm^{-1}, the latter somewhat broadened on the low-frequency side. Upon evacuation of CO (spectra 2a and 2b) only the band at 2040 cm^{-1} remains on both samples, the forms of adsorbed CO contributing to the high-frequency bands having been removed.

An illustration of the conversion of an oxidized Ru sample back to a reduced state is shown in Fig. 10. CO was first adsorbed at 25°C on an oxidized sample (spectrum 2), and then the sample was

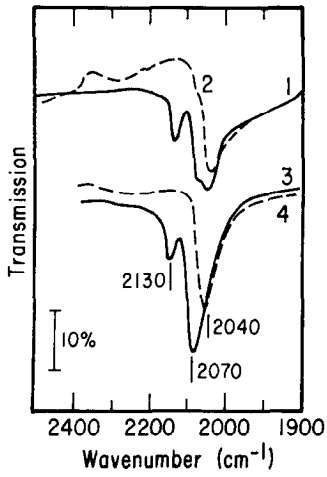

FIG. 9. Spectra of CO adsorbed in Ru: (1) following oxidation in N_2O at 23 Torr and 25°C, evacuation of N_2O at 25°C, and adsorption of CO at 10 Torr and 25°C; (2) following evacuation of CO at 25°C; (3) following oxidation in NO at 10 Torr and 25°C, evacuation of NO at 300°C, and adsorption of CO at 15 Torr and 25°C; (4) following evacuation of CO at 25°C.

heated in stages up to 300°C (spectra 3 and 4). Notice that spectrum 2 is characteristic of CO adsorption on an oxidized sample. As the temperature increases the spectra change toward those characteristic for CO adsorption on a reduced sample.

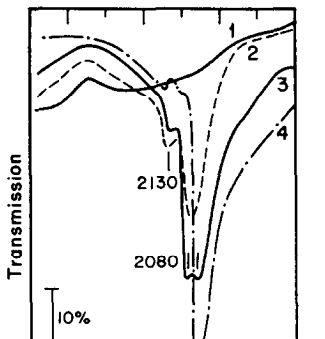

FIG. 10. Spectra of CO adsorbed on Ru: (1) background; (2) following adsorption of CO at 44 Torr and 25°C; (3) following heating for 1 hr in CO at 200°C; (4) following heating for 1 hr in CO at 300°C.

Finally, we note that experiments were also carried out using ^{13}CO. The results were essentially identical to those obtained using ^{12}CO with the exception that the bands occurring at 2130, 2070, and 2040 cm^{-1} were shifted to 2100, 2030, and 1990 cm^{-1}.

DISCUSSION

Molecular Bonding in Transition Metal Carbonyls and Nitrosyls

Prior to interpreting the spectra obtained in this study it will be useful to review briefly the molecular orbital description of bonding in transition-metal complexes involving carbonyl or nitrosyl groups and the effect of coordination on the ligand vibrational frequency. The M–C or M–N bond in such complexes is composed of a dative σ bond and a dative π bond which produce charge shifts in opposite directions. The σ bond is formed by electron transfer from the filled 5σ orbital of either CO or NO to an unfilled d orbital on the metal. The π bond results from back donation of electrons from filled d orbitals on the metal into the anti-bonding π^* orbitals of the ligand. This view of bonding in transition-metal carbonyls and nitrosyls has been extended by Blyholder (*9*) to explain the adsorption of CO and NO or transition metals.

The electronic structures of uncoordinated CO and NO are similar, with the exception that the $2\pi^*$ orbital is empty for CO and contains one electron for NO. This difference in the electronic structure leads to an important difference in the bonding characteristics of NO and CO. Whereas CO usually coordinates as the neutral molecule, experimental evidence indicates that many NO complexes are best viewed as involving first a transfer of an electron from the NO to the metal atom, followed by coordination of the resulting NO^+ (*10*). Coordination of nitric oxide as NO or NO^- can also occur but these forms are infrequently observed in complexes involving ruthenium (*11*).

The process involved in the formation of the σ and π bonds between metal and ligand lead to a cooperative strengthening of the metal–ligand bond. At the same time, back donations of electrons into the $2\pi^*$ anti-bonding orbital of the ligand cause a slight weakening of this bond between the two atoms of the ligand. The presence of additional ligands on the metal can also influence the bonding between the metal and either the carbonyl or nitrosyl group. Thus, strongly electronegative ligands will reduce the ability of the metal to provide d electrons for back bonding and will result in a weakening of the metal–ligand bond and a strengthening of the bond between the atoms comprising the ligand. The opposite effects are obtained when electropositive ligands are present.

Interpretation of the Spectra of Adsorbed NO

The infrared spectra of adsorbed NO show two principle features, a low-frequency band at 1810 cm^{-1} and a high-frequency band at 1860 cm^{-1}. With prolonged exposure to NO at high temperatures, the high-frequency band shifts to 1880 cm^{-1}. For the purpose of assigning structures to these features it is desirable to examine first the forms in which NO is coordinated in Ru–nitrosyl complexes. Listed in Table 1 are the N–O stretching frequencies for a number of representative complexes. Following the classification of Lewis *et al.* (*12*), vibrational frequencies between 1980 and 1580 cm^{-1} can be assigned to NO coordinated in the form of NO^+ and frequencies between 1580 and 1045 cm^{-1} to NO coordinated in the form of either NO^-, $-NO$, or $\diagdown\!\!\diagup NO$. Consistent with this classification, the NO bands in $Ru(NO)(CO)(PPh_3)Cl$ are assigned to $-NO$, the band in $Ru_3(NO)_2(CO)_{10}$ is

TABLE 1

NO Vibrational Frequencies in Ruthenium Nitrosyls

Compound	ν_{NO} (cm^{-1})	Ref.	Compound	ν_{NO} (cm^{-1})	Ref.
$Ru_2O_5(NO)_4(NO_3)_2$	1976	(*10*)	$K_2[Ru(NO)(CN)_5]$	1916	(*17*)
$Ru(NO)Cl_3$	1916	(*10*)	$K_2[Ru(NO)(Cl)_5]$	1910	(*17*)
$Ru(NO)(dipy)Cl_3$	1886, 1879	(*11*)	$K_2[Ru(NO)(Br)_5]$	1875	(*17*)
$Ru(NO)(o\text{-phen})Cl_3$	1882, 1874	(*11*)	$K_2[Ru(NO)(I)_5]$	1840	(*17*)
$Ru(NO)(PPh_3)Cl_3$	1876	(*11*)	$[Ru(NO)(NH_3)_4(NH_3)]Cl_3$	1903	(*18*)
$Ru(NO)(AsPh_3)Cl_3$	1874	(*11*)	$[Ru(NO)(NH_3)_4(Cl)]Cl_2$	1880	(*18*)
$Ru(NO)(das)Cl_3$	1865	(*11*)	$[Ru(NO)(NH_3)_4(Br)]Br_2$	1870	(*18*)
$Ru(NO)(Pyr)Cl_3$	1853	(*11*)	$[Ru(NO)(NH_3)_4(I)]I_2$	1860	(*17*)
$Ru(NO)(SbPh_3)Cl_3$	1833	(*11*)	$Ru(NO)(CO)(PPh_3)Cl$	1517, 1500	(*11*)
$Ru(NO)(PEt_3)_2Cl_3$	1829	(*11*)	$Ru_3(NO)_2(CO)_{10}$	1592	(*11*)

assigned to $\diagdown$ NO, and the bands for the $\diagup$ remaining complexes are assigned to NO^+.

The vibrational frequency of the coordinated NO^+ group is influenced by the nature of the other ligands present in the coordination sphere. When strongly electrophilic groups are present, d electrons are drawn away from the Ru atom, thereby causing a reduced back donation of these electrons into the Ru–N bond. Under these circumstances the N–O bond is strengthened, and its vibrational frequency is shifted toward that of gas-phase NO^+. If electron-donor groups are present in addition to electron-acceptor groups, the availability of d electrons for back bonding increases, and the N–O frequency is shifted to lower values.

Comparison of the vibrational frequencies for adsorbed NO with those for NO in Ru complexes strongly suggests that NO is adsorbed as NO^+. An interpretation of the occurrence of two bands and the shift of the high-frequency band can be envisioned in the following manner.

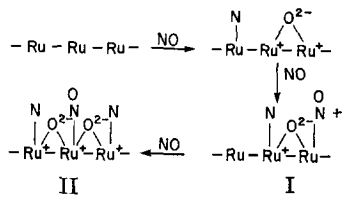

Initial adsorption of NO onto a reduced surface results in the dissociation of the NO and the production of oxidized sites. The occurrence of this step is supported by our observations that NO will readily oxidize a reduced Ru surface at 25°C. Similar observations have been made by Ku *et al.* (*13*) for NO adsorption on a $10\bar{1}0$ Ru surface. We will identify the oxidized sites produced by the initial dissociative adsorption as type I sites. Adsorption of NO on type I sites would be expected to occur with the transfer of an electron from the NO molecule to the partially ionized site. Such a transfer would have the effect of strengthening both N–O and Ru–N bonds, the former through the removal of anti-bonding character from the N–O bond and the latter through the increase of Ru d electrons available for back bonding. Further oxidation of the surface as a result of prolonged exposure to NO is postulated to produce type II sites. NO adsorption at type II sites should also be possible and, again, would be expected to produce NO^+-adsorbed species.

With the above picture in mind, we have assigned the bands observed at 1810–1815 cm^{-1} to NO^+ cations associated with type I sites and the bands observed at 1860–1880 cm^{-1} to NO^+ cations present on type II sites. The higher vibrational frequency of the NO adsorbed on type II sites is a

direct reflection of the lesser availability of Ru d electrons at these sites, relative to that available at type I sites. As is evident upon inspection of Table 1, increasing withdrawal of Ru and d electrons causes a strengthening of the $N-O^+$ bond and a consequent increase in the N–O bond vibrational frequency. The rather broad range of frequencies associated with NO adsorbed at type II sites probably reflects the number of O^{2-} anions present in the coordination sphere of the Ru atom constituting the site. The larger the number of anions per site the greater should be the frequency of the adsorbed NO^+ cation.

Consistent with the proposed interpretation, one would expect the Ru–N bond to be weaker for NO adsorbed on type II sites than that adsorbed on type I sites. Evidence supporting this expectation can be found in Fig. 1 which shows that desorption occurs at lower temperatures from type II sites than from type I sites.

Interpretation of the Spectra of Adsorbed CO

Carbonyl stretching frequencies for a number of Ru complexes are listed in Table 2. In all of these compounds the carbonyl groups are present only in terminal positions since bands with frequencies below 1900 cm^{-1}, characteristic of bridging carbonyls, are absent (*8*). Shifts in the vibrational frequencies relative to those associated with $Ru(CO)_5$ can be interpreted in terms of changes in the extent of d-electron back bonding. The higher frequencies characteristic of $Ru_3(CO)_{12}$ are the result of the reduced availability of d electrons due to formation of Ru–Ru bonds. A similar effect has been noted for Pt–carbonyl clusters of increasing size (*14*). Introduction of electrophilic ligands into the coordination sphere also causes a withdrawal of d electrons and results in an increase in the C–O frequencies. This effect is particularly noticeable for the halocarbonyls and increases with increasing electronegativity of the halogen. When both electrophilic and electrophobic ligands are present, as in the case of $Ru(CO)_2(Pyr)_2Cl_2$, the C–O frequencies are shifted downscale relative to those observed when only electrophilic groups are present. This trend reflects the ability of the pyridine groups to compensate for the withdrawal of d electrons by the chlorine atoms.

The number of strong or moderate intensity bands associated with each complex reflects the relative positions of the carbonyl groups. The second column in Table 2 illustrates the disposition of the carbonyl groups around each Ru atom and the third column indicates the number of infrared active bands predicted on the basis of symmetry arguments (*15*). A single band is observed when only a single carbonyl group is present or when all of the carbonyl groups are arranged along a line of symmetry or in a plane of symmetry. Two bands are observed when two carbonyl groups are present, arranged *cis* to each other. Finally, three bands are observed when two or more carbonyl groups are disposed *cis* to each other in a plane, and additional groups are present along an axis which is perpendicular to the plane.

In the presence of gas-phase CO the spectrum of CO chemisorbed on a fully reduced Ru surface shows only a single band at 2040 cm^{-1}. By comparison with Table 2 it seems reasonable to assign this band to a structure of the form Ru–C=O. The shift in frequency of the band from 2040 to 2030 cm^{-1} upon evacuation of the gas phase and the further shift to 2010 cm^{-1} upon heating under vacuum can be explained most reasonably in the following manner. With decreasing surface coverage the availability of Ru d electrons for back bonding increases. This contributes to a strengthening of the Ru–C bond and a weakening of the C–O bond for the CO still chemisorbed on the surface of the catalyst. The latter effect causes a decrease in the vibrational frequency of the C–O bond.

TABLE 2

CO Vibrational Frequencies in Ruthenium Carbonyls

Compound	Orientation of CO groups	Number of CO bonds	ν_{CO} (cm^{-1})	Ref.
$Ru(CO)_5$		2	2035 s, 1999 s	(*19*)
$Ru_3(CO)_{12}$		3	2059 s, 2029 ms, 2010 min	(*20*)
$Ru(CO)_4Cl_2$		3	2182, w, 2132 s, 2113 ms, 2080 s	(*21*)
$Ru(CO)_4Br_2$		3	2178 w, 2124 s, 2110 m, 2078 m	(*21*)
$Ru(CO)_4I_2$		3	2160 w, 2105 s, 2095 m, 2066 m	(*19*)
$[Ru(CO)_2Cl_2]_2$		3	2140 s, 2092 s, 2066 s	(*21*)
$[Ru(CO)_3Br_2]_2$		3	2139 , 2078 s, 2067 s	(*21*)
$Ru(CO)_3(Pyr)Cl_2$		3	2136 s, 2075 s, 2051 s	(*21*)
$Ru(CO)_2(Pyr)_2Cl_2$		2	2070 s, 2006 s	(*21*)
$Ru(CO)_4(PF_3)$		1	2106 w, 2087 w, 2041 s, 2027 w	(*22*)
$Ru(CO)_3(PF_3)_2$		1	2084 vw, 2071 mw, 2041 s, 2026 w	(*22*)
$Ru(CO)_2(PF_3)_3$		1	2078 w, 2038 s, 2026 w, 2007 vw	(*22*)
$Ru(CO)(PF_3)_4$		1	2070 s, 2026 w	(*22*)

On a partially or fully oxidized surface CO adsorption produces two bands, which occur at 2140 and 2080 cm^{-1} in the former case and at 2130 and 2070 cm^{-1} in the latter case. Inspection of Figs 6 through 9 reveals that the intensities of the two bands appear to change in parallel during CO desorption, suggesting that both bands are associated with a single form of adsorption. It is important to note that our observations differ from those of Dalla Betta (*4*) and Brown and Gonzalez (*5*). In both studies it was concluded that the higher-frequency band desorbed more readily than the lower-frequency band. The significance of this conclusion must be questioned, however, since it was based on either very weak spectra (*4*) or spectra in which the lower frequency band was poorly resolved from a band occurring near 2040 cm^{-1} (*5*).

Reference to Table 2 shows that the frequencies of the CO bands observed on oxidized Ru agree most closely with those for C–O vibrations in halocarbonyls. This correspondence strongly implies that the adsorption site is partially ionized, most probably as a result of its association with oxygen. Furthermore the observation of a pair of bands whose intensities are correlated suggest that there are two CO molecules adsorbed at each site, as shown below.

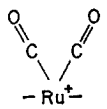

This type of structure would be expected to produce two infrared bands, corresponding to symmetric and asymmetric stretches of the carbonyl groups.

The model of carbonyl bonding outlined earlier, predicts that structures characterized by high C–O frequencies should be more weakly bound to the surface than structures characterized by low C–O fre-

quencies. This prediction is consistent with our observations since we recall that CO adsorbed on reduced Ru sites is not readily desorbed upon evacuation at 25°C, while a part of the CO adsorbed on oxidized Ru sites is easily desorbed (see Fig. 5).

In addition to providing an explanation for the spectra reported here the proposed structures for chemisorbed CO can be used to reinterpret the spectra reported by Dalla Betta (*4*). We recall first that, for Ru particles less than 60 Å in diameter, Dalla Betta observed three infrared bands at frequencies similar to those reported here. The low-frequency (LF) band was assigned to CO adsorbed on low-index faces of Ru and the medium- and high-frequency (MH and HF) bands were assigned to CO adsorbed on low-coordination sites or sites adsorbing more than one CO molecule. These assignments led Dalla Betta to conclude that CO adsorption on Ru did not follow Blyholder's (*9*) molecular orbital description of CO bonding to transition metals, which predicts lower C–O vibrational frequencies for CO attached to low-coordination sites than for CO attached to high-coordination sites. The disagreement can easily be resolved if it is postulated that the MF and HF bands are characteristic of adsorption on oxidized Ru sites and that the higher frequencies are the result of a decrease in availability of d electrons. Dalla Betta's (*4*) observation that the frequencies and intensities of the MF and HF bonds change in concert with Ru particle size provides additional support for our assignment of these bands to a single surface structure.

We note further that Dalla Betta observed an increase in the intensities of the MF and HF bands relative to the LF band and an increase in the ratio of CO molecules adsorbed per Ru site as a result of decreasing Ru particle size. This trend suggests that the smaller particles were more highly oxidized than the larger ones and that, consistent with our proposed structures, multiple CO adsorption occurred preferentially on the oxidized sites. At least two explanations can be offered for the occurrence of higher degrees of oxidation for the smaller particles. The first is that such particles retain oxygen on their surface which is not readily removed, even upon exposure of the catalyst to H_2 at high temperatures (viz. 450°C). The second explanation is associated with the possibility of electron transfer from the Ru particles to Lewis acid sites on the alumina support (*8*). Smaller particles would be expected to reflect the effects of such transfer more extensively than larger ones (*16*).

CONCLUSIONS

Our observations have shown that the initial adsorption of NO onto a fully reduced Ru surface occurs dissociatively and results in a partial oxidation of the surface. Subsequent adsorption occurs both dissociatively and associatively, the latter producing NO^+ adspecies. The molecularly adsorbed NO is characterized by two infrared bands. The first is observed at 1810 cm^{-1} and is associated with NO adsorbed at partially oxidized sites. The second band is observed at 1860 to 1880 cm^{-1} and is assigned to NO adsorbed on fully oxidized sites. The position of the high-frequency band correlates with the extent of surface oxidation. As the extent of oxidation increases, the band shifts to higher frequencies.

Carbon monoxide adsorption also occurs in different forms, depending upon whether the Ru surface is reduced or oxidized. On a fully reduced sample, evidence from infrared spectra suggests that only a linearly bonded form is present. This species is characterized by a band at 2040 cm^{-1}. On a fully oxidized surface a pair of bands are observed at 2130 and 2070 cm^{-1}, which are assigned to the symmetric and asymmetric vibrations of a pair of CO molecules adsorbed on a common Ru^+ site.

The infrared bands observed for adsorbed NO and CO agree very closely with those reported in the literature for ruthenium nitrosyls and carbonyls. The observed upscale shift in adsorbate vibrational frequency and the weakening of the adsorbate–metal bond which occur upon oxidation of the adsorption site are consistent with a molecular orbital interpretation of adsorption. Based upon this model the adsorbate–metal bond is composed of dative σ and π bonds. Reducing the availability of d electrons at the adsorption site as a result of oxidation results in a weakening of the adsorbate–metal bond and a concurrent strengthening of the bond between the atoms comprising the adsorbate, i.e., NO or CO.

ACKNOWLEDGMENT

This work was supported by the U. S. Energy Research and Development Administration and by the National Science Foundation (Grant GP-43728)

REFERENCES

1. Lynds,L., *Spectrochem. Acta* **20**, 1369 (1964).
2. Guerra, C. R., and Schulman, J. H., *Surface Sci.* 229 (1967)
3. Kobayashi, M., and Shirasaki, T., *J. Catal.* **28**, 289 (1973)
4. Dalla Betta, R. A., *J. Phys. Chem.* **79**, 2519 (1975).
5. Brown, M. F., and Gonzalez, R. D., *J. Phys. Chem.* **80**, 1731 (1976).
6. Unland, M. L., *Science* **179**, 567 (1973).
7. Brown, M. F., and Gonzalez, R. D., *J. Catal.* **44**, 477 (1976).
8. Little L. H., "Infrared Spectra of Adsorbed Species." Academic Press, New York, 1966.
9. Blyholder, G., *J. Phys. Chem.* **68**, 2772 (1964); Blyholder, G., and Allen, M. C., *J. Amer. Chem. Soc.* **91**, 3158 (1969).
10. Johnson, B. F. G., and McCleverty, J. A., *in* "Progress in Inorganic Chemistry" (F. A. Cotton, Ed.), p. 277. Interscience, New York, 1966.
11. Connelley, N. G., *Inorg. Chem. Acta Rev.* **47** (1972).
12. Lewis J., Irving, R. J., and Wilkinson, G., *J. Inorg. Nucl. Chem.* **7**, 32 (1958); Griffith, W. P., Lewis, J., and Wilkinson, G., *J. Inorg. Nucl. Chem.* **7**, 38 (1958).
13. Ku, R., Gjostein, N. A., and Bonzel, H. P., *in* "The Catalytic Chemistry of Nitrogen Oxides" (R. L. Klimisch and J. G. Larson, Eds.). Plenum Press, New York, 1975.
14. Primet, M., Bosset, J. M., Grabowski, E., and Mathieu, M. V., *J. Amer. Chem. Soc.* **97**, 3655 (1975).
15. Nakamoto, K., "Infrared Spectra of Inorganic and Coordination Compounds," 2nd ed. Wiley–Interscience, New York, 1970.
16. Hulse, J. E., and Moskovits, M., *Surface Sci.* **57**, 125 (1976).
17. Murrell, J. N., and Nikolskii, A. B., *J. Chem. Soc. (A)* 1363 (1970).
18. Schreiver, A. F., Liu, S. W., Hauser, P. J., Hopcus, E. A., Hamm, D. J., and Gunter, J. D., *Inorg. Chem.* **11**, 880 (1972).
19. Calderazzo, F., and L'Eplattenier, F., *Inorg. Chem.* **6**, 1220 (1967).
20. Bruce, M. I., and Stone, F. G. A., *Angew. Chem. Int. Ed.* **1**, 427 (1968).
21. Benedetti, E., Braca, G., Sbrana, G., Salvetti, F., and Grassi, B., *J. Organometal. Chem.* **37**, 361 (1972).
22. Udovich, C. A., and Clark, R. J., *J. Organometal. Chem.* **36**, 355 (1972).